DT-NMBP-08-2019
Real-time nano-characterisation technologies

NanoQI

Multimodal X-ray and Hyperspectral Thin-Film Nano-material Evaluation and Quality Imaging

Starting date of the project: 01/03/2020
Duration: 42 months

= Deliverable D6.1 =

Verification of in-situ observation of perovskite layer curing and quenching and surface imaging on > 20 x 20 cm² on moving substrate (0.5 m/min)

Due date of deliverable: 31/08/2023
Actual submission date: 01/09/2023

WP and Lead Beneficiary: WP6, Nordmeccanica (NORD)
Version: V1.0

Dissemination level		
PU	Public	X
CO	Confidential, only for members of the consortium (including the Commission Services)	
CI	Classified, information as referred to in Commission Decision 2001/844/EC	

This project has received funding from the European Union's Horizon 2020 research and innovation programme under grant agreement No 862055.

AUTHOR

Author	Organization	Contact (e-mail, phone)
Giulia Lucarelli	TNO	giulia.lucarelli@tno.nl
Harrie Gorter	TNO	Harrie.gorter@tno.nl

DOCUMENT DATA

Keywords	HSI, XRD, perovskite solar cells, large area slot die coating
Point of Contact	Giulia Lucarelli (TNO) giulia.lucarelli@tno.nl

DISTRIBUTION LIST

Date	Issue	Recipients
30/08/2023	V0.1	Sjoerd Veenstra (TNO), Klaas Bakker (TNO), Jos Bakema (STS), Alexander Kabardiadi-Virkovski (FhG-IWS), Raffaele Guadagno (NORD), Fabiano Rimediotti (NORD), Julio Hernandez (NEO), Dennis Adamek (NEO), Matthias Fahland (FEP), Martina Chopart (AMI)
01/09/2023	V1.0	EC, Partners

REVIEW PROCESS

Document version	Date	Status/Change
V0.1	30/08/2023	All measurements integrated into first draft report
V1.0	01/09/2023	Feedback from partners and Coordinator incorporated, formatted

VALIDATION PROCESS

Reviewers		Validation date
Work Package Leader	Fabiano Rimediotti (NORD)	31/08/2023
Project Manager	Martina Chopart (AMI)	01/09/2023
Project Coordinator	Matthias Fahland (FEP)	31/08/2023

Executive Summary

The NanoQI analytical tool, composed of hyperspectral imaging (HSI) and x-ray-diffraction (XRD) setups, is validated and demonstrated in the perovskite pilot line for characterization of perovskite films on substrate size up to 30 cm x 40 cm:

- speed of 0.5 m/min and imaging size > 20 cm x 20 cm were demonstrated for two different HSI setup configurations covering the VNIR (visible near infrared) and SWIR (short wavelength infrared) wavelength range (400 nm to 2500 nm);
- measurement speed of the Proto-T XRD unit was assessed and the accuracy over large areas was verified.

Quenching of slot die coated samples was imaged in-situ in real time with the SWIR and VNIR cameras simultaneously. Films with variation in characteristic properties were fabricated and analysed with the HSI and XRD tools. Properties of interest included thickness, roughness and phase composition. To induce phase composition variations, quenching and annealing variations, controlled ageing and suboptimal deposition parameters were investigated. Using software suites from NEO, quantification models were successfully built to correlate:

- sample thickness and roughness to VNIR and SWIR HSI data;
- intensity of selected XRD peaks to the VNIR and SWIR HSI data.

Finally, solar cells were fabricated, and a tentative model was developed to correlate photovoltaic parameters to the HSI signal of the cells.

Table of Contents

1. Introduction 5
2. Results and discussion 6
2.1. Setup description and validation of HSI and XRD tools 6
2.2. In-situ imaging of perovskite quenching 11
2.3. Thickness and roughness models 14
2.4. Composition model 16
2.5. Solar cell fabrication and evaluation 21
3. Conclusions 24
4. Degree of progress 25
5. Dissemination level 25
6. References ..... Error! Bookmark not defined.
7. Appendix 1 ..... Error! Bookmark not defined.

1. Introduction

Deliverable 6.1 describes the validation and demonstration of hyperspectral imaging (HSI) and x-ray diffraction (XRD) analytical tools for process and quality control in perovskite solar cell manufacturing. The XRD and HSI hardware and software that were installed and commissioned in WP5, are used in Task 6.1 to evaluate characteristic properties of perovskite coatings, such as thickness, roughness and phase composition. Partial least square regression (PLS) quantification models are developed to correlate the in-line HSI signals with the film properties.

Perovskite films are deposited on 30 cm x 40 cm glass substrates by slot die coating of the precursors ink, followed by vacuum quenching and thermal annealing in a semi-automated pilot line. Hyperspectral images are recorded during the film quenching and after a complete curing cycle (quenching and subsequent annealing). XRD spectra are measured after complete curing of the samples on several points of the sample. Thickness and roughness are measured by means of off-line techniques.

By incorporating the perovskite layers characterized with the NanoQI tools in a complete p-i-n device architecture, semitransparent solar cells were fabricated and their photovoltaic parameters were determined with a solar simulator at standard testing conditions.

2. Results and discussion

2.1. Setup description and validation of HSI and XRD tools

To validate the use of HSI and XRD characterization tools for quality control in perovskite solar cell manufacturing, tests were carried out at TNO in the sheet-to-sheet (S2S) pre-pilot line equipped with a large area ambient slot die coater connected to vacuum quenching unit and a modular curing oven. Substrate size is 30 cm x 40 cm. Typical coating size is 29 cm x 30 cm. Coating width is limited by the geometry of the slot die coating head.

HSI measurements were carried out with a double camera configuration, allowing simultaneous imaging in the (visible near infrared) VNIR and short wavelength infrared (SWIR) range. The first set of experiments was performed with the HySpex-SWIR384 and the Baldur-V-1024N cameras. The second set of experiments was performed with the HySpex-SWIR384 and the HySpex-VNIR1800 cameras (Figure 1). An overview of the performance parameters of the two configurations, together with optimal imaging settings used in the tests and achievable sample speed are reported in Table 1.

Image acquisition and processing was done via software suites provided by NEO, as the ImantoPro software suite was not (and not intended to be) implemented within the project duration time to acquire signals from multiple cameras simultaneously. Image acquisition was done with HySpex Ground software. After recording sample images, at intervals of approx. 1-2 hours, an image of the white background reference foil was also recorded. Raw data of perovskite samples was corrected by the reference background image via the HySpex Rad software. For data visualization GLIMPS was used. The white reference foil provided by FhG-IWS was also used as carrier for the coatings: perovskite-coated glass samples were manually attached/detached to/from the white reference foil adhered to a glass substrate before every quenching/annealing cycle as the robotic arm is not programmed to work with samples of unusual format and to avoid damage of the foil at high temperatures.

Table 1. Parameters and settings of the HSI setup in the perovskite S2S pilot line

SWIR384 + Baldur-V-1024N		
	SWIR384	Baldur-V-1024N
Field of view (mm)	289	283
Lateral resolution (mm)	0.75	0.65
Frame period (ms)	10003	3700
Integration time (ms)	8500 / 9500	3599 / 3400
Sample speed (mm/s)	80 / 77	
SWIR384 + VNIR1800		
Field of view (mm)	289	285
Lateral resolution (mm)	0.75	0.29 (at 452 nm)
Frame period (ms)	54749	11999
Integration time (ms)	12500	11997
Sample speed (mm/s)	14	

a)  b) 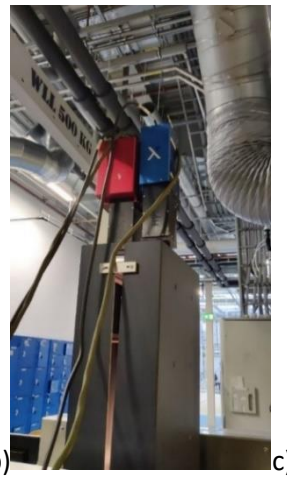 c) 

Figure 1. HSI setup installed on top of the vacuum chamber of the perovskite pilot line, in three configurations: a) SWIR only, b) SWIR + Baldur V-1024N, c) SWIR + VNIR1800.

The speed target defined in the deliverable (0.5 m/min = 8.33 mm/s) is achieved with both configurations. The sample speed must be defined depending on the camera and imaging settings, according to the following formula:

Belt speed [mm/s] = (FOV [mm] / # pixels) / frame period [s]

FOV and number of pixels are defined by the setup and type of camera. The frame period must be adjusted to maximise the HSI signal intensity. Frame periods of the two cameras are linked. Integration time must be as close as possible to the frame period; this parameter also affects signal intensity. Incorrect sample speed results in image distortion. For both double camera configurations, a frame period compatible with sample speeds higher than 8.33 mm/s could be used without compromising the signal intensity and image quality.

Size requirements area also (partially) achieved. The line equipped with HSI and XRD tool is designed and operates with 30 cm x 40 cm substrates; the coated area is 29 cm x 30 cm. Imaged area with the HSI systems is approx. 28 cm x 12 cm due to geometrical constraints in the system: the sample is imaged while moving back and forth for a defined time inside a closed vacuum chamber of 50 cm length in the transport direction.

The Prototype-T, installed and validated in WP5 (D5.1, D5.3), was used for XRD analysis of the large area coating. First, the measurement speed and accuracy of the signal were verified on large areas.

For the former, measurements were done at various speeds and using 2 divergent slit settings (either for 5 or 30 mm length sample irradiation) using the c reference sample in the small sample holder attached to the large sample table. Time per step setting t_s was varied between the shortest value of 0.005 and 1 second, with an angular (2θ) step size of 0.01326°. In the set-up with the goniometer radius of 520 mm, the detector scans simultaneous a range of 1.5912°, so the total measurement time t_m of a measurements is:

$$t_m = ((\#steps/scan) + (1.5912/ 0.01326)) * t_s$$

Figure 2 shows XRD patterns of the National Institute of Standards and Technology (NIST)-certified reference material SRM1976c measured at various speeds at illuminated lengths (IL) of either 5 or 30 mm. The peak intensity decreases with higher measurement speed; intensities are also lower for the shorter illuminated length. At the highest measured speed of 156°/min most peaks are still detected, except for a few very weak reflections; the pattern between 5 and 90° is measured within 33 seconds. The fingerprint range for perovskite samples is between 7 and 15°, which can be measured at such speed within 0.65 seconds.

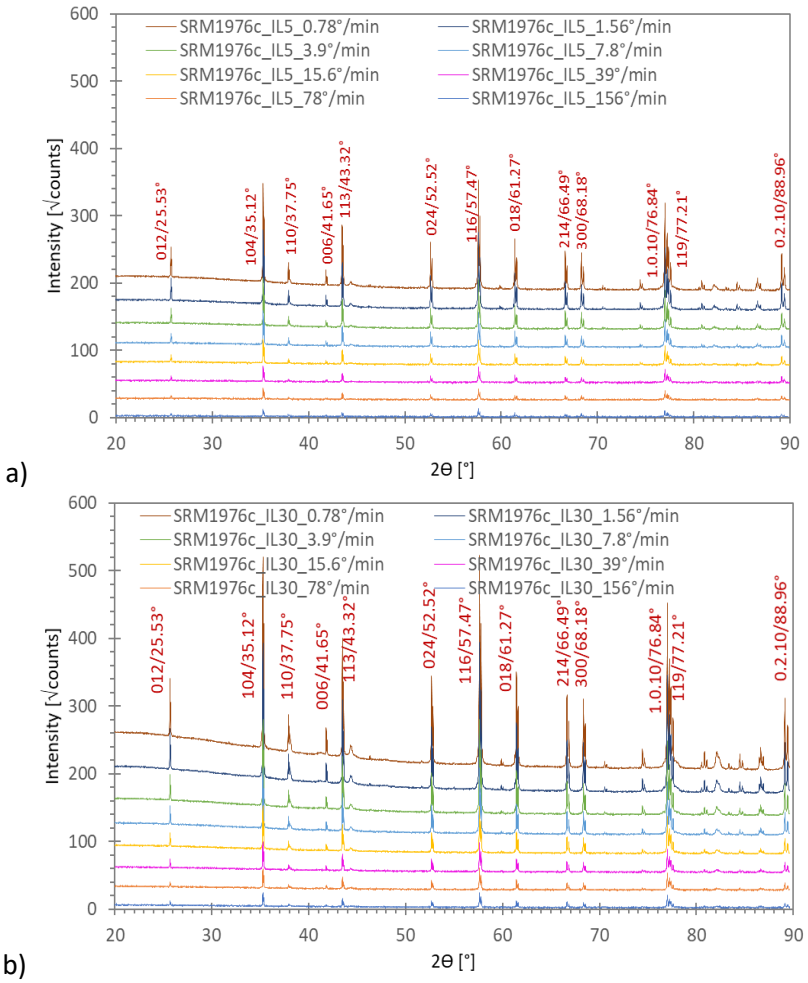

Figure 2. XRD pattern of SRM1976c at different measurement speeds for illuminated lengths of a) 5 and b) 30 mm.

The signal-to-noise ratio (SNR) is approximated here by dividing the peak height by the square root of the background level. In Figure 3, the SNR are given for several peaks as a function of measurement speed. Assuming we want the S/N ratio to remain above an arbitrary value of 20, then for both IL values, the speed should remain below app. 40°/min. At this speed, the fingerprint region of perovskite samples can be scanned within 2.6 seconds.

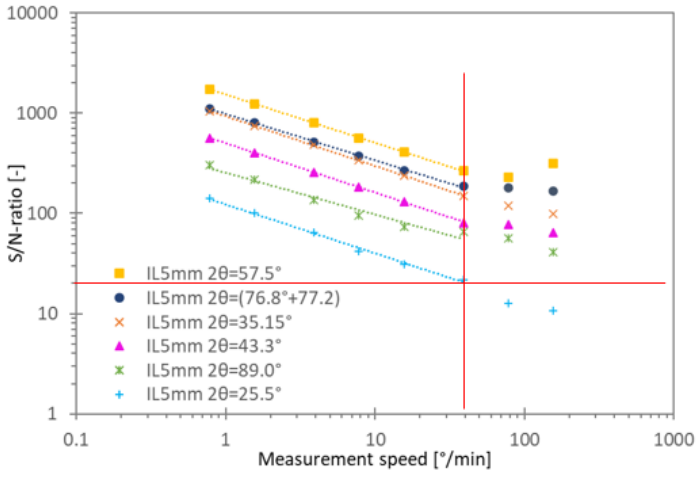

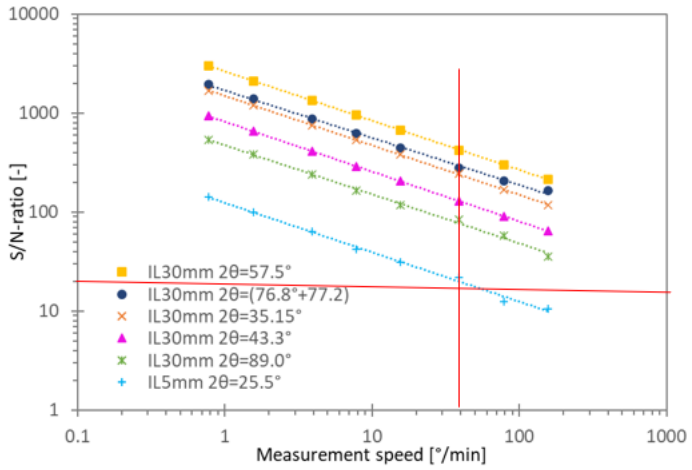

b)

Figure 3. Signal-to-noise ratio of SRM1976c reflection peaks as a function of the measurement speed for illuminated lengths of a) 5 and b) 30 mm.

In XRD, resolution is dependent on the peak width. In Figure 4 the full width at half maximum (FWHM) is reported for both IL values. FWHM increases by 5-10% for a 6-fold increase in IL. It is almost independent of speed up to at least 15°/min for the IL of 5 mm; at 30 mm IL the maximum speed is app. 40°/min.

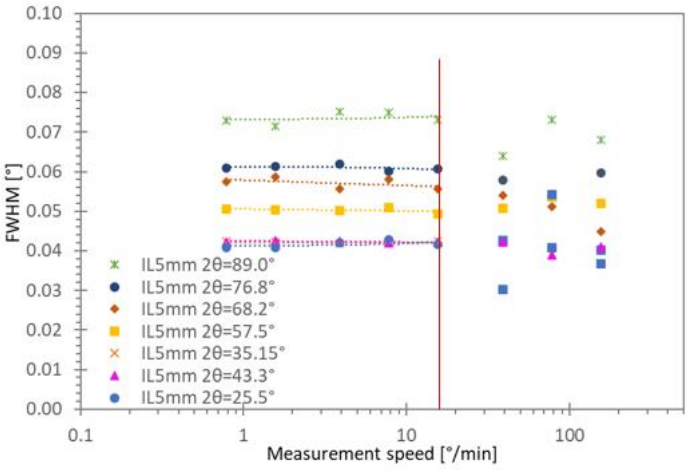

a)

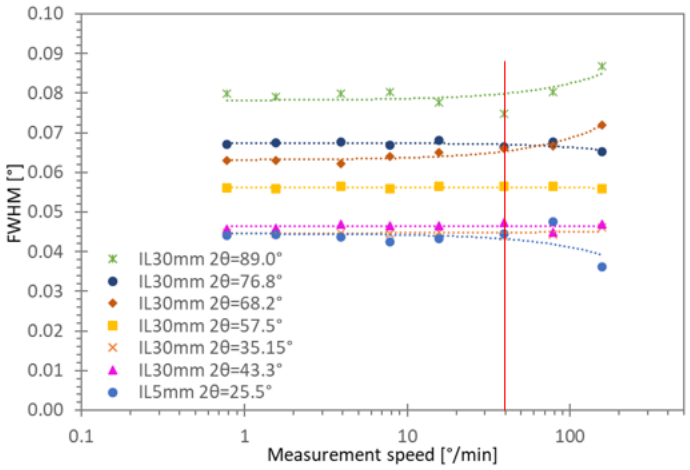

b)

Figure 3. Full width at half maximum of SRM1976c reflection peaks as a function of the measurement speed for illuminated lengths of a) 5 and b) 30 mm.

Therefore, the measurement speed can be increased to 40°/min, when using an IL of 30 mm, and 15°/min at 5 mm IL. For IL= 30 mm the fingerprint area for Perovskite of 2θ=7-15° can be measured reliably in 2.6 seconds and an extend region of 2θ=7-60° can be measured in 3.5 s. For an illuminated length of 5 mm the fingerprint area for

Perovskite of 2θ=7-15° can be measured reliably in 6.4 seconds and an extend region of 2θ=7-60° can be measured in 8.7 s. The measured loading time for a sample to the measurement position is app. 30-35 s; unloading takes about the same time. Measurement time will depend also on the number of points of the samples to be analysed. Therefore, the Proto-T gives enough flexibility to increase the measurement speed according to the requirements of the manufacturing process.

The Proto-T XRD unit can scan along a line over a substrate. By moving the table along the X-direction, a measurement can be done at various locations of a coated plate. The maximum travel distance for the table is from -152 to +152 mm, so in total 304 mm. The accuracy of the measurements was tested by measuring Tb-doped Gd_2O_2S (Mitsubishi Scintillator Screen, MSS), SRM1976c and a slot die coated perovskite sample at various X-positions, using the Z-position zero-correction determined for position X= 0 mm. In Figure 4, the average error in Z-height for each X-position, for both the SRM1976c, Gd_2O_2S and perovskite are reported. The Z-error of the measurement is within ±0.1 mm and follows the same parabolic trend for the three samples analysed. These results indicate that the error is most likely caused by a small positional offset during the X-movement and that offset is reproducible.

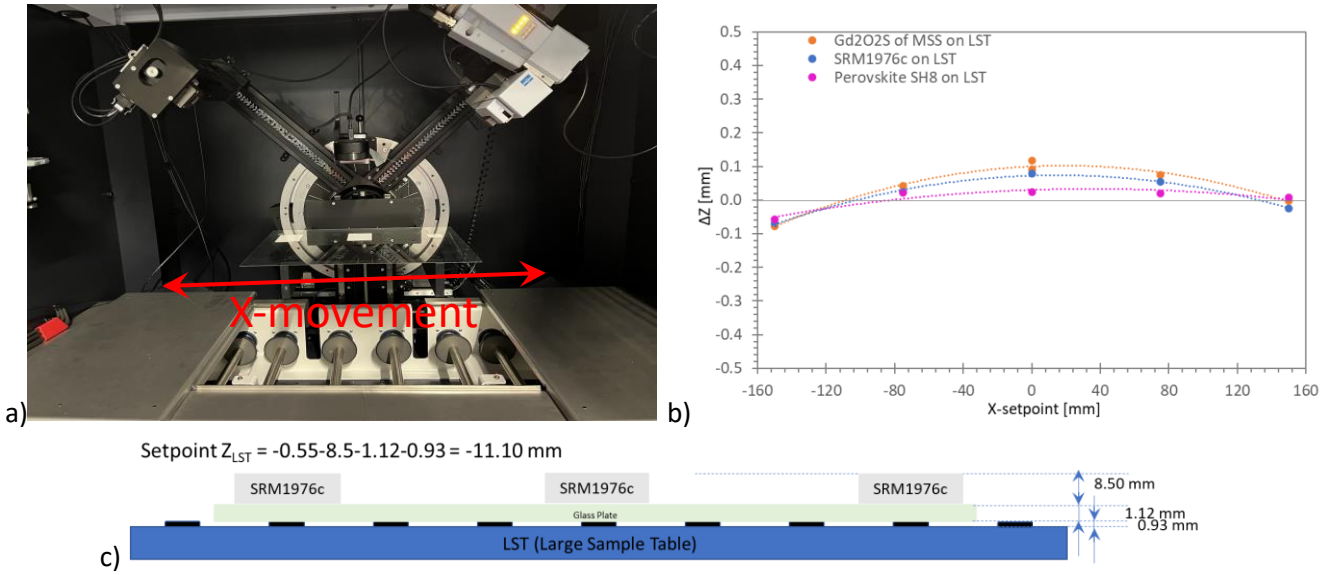

Figure 4. Image of XRD tool highlighting the x-movement direction; error in Z-height for each X-position, for both the SRM1976c, Gd_2O_2S and perovskite are reported.

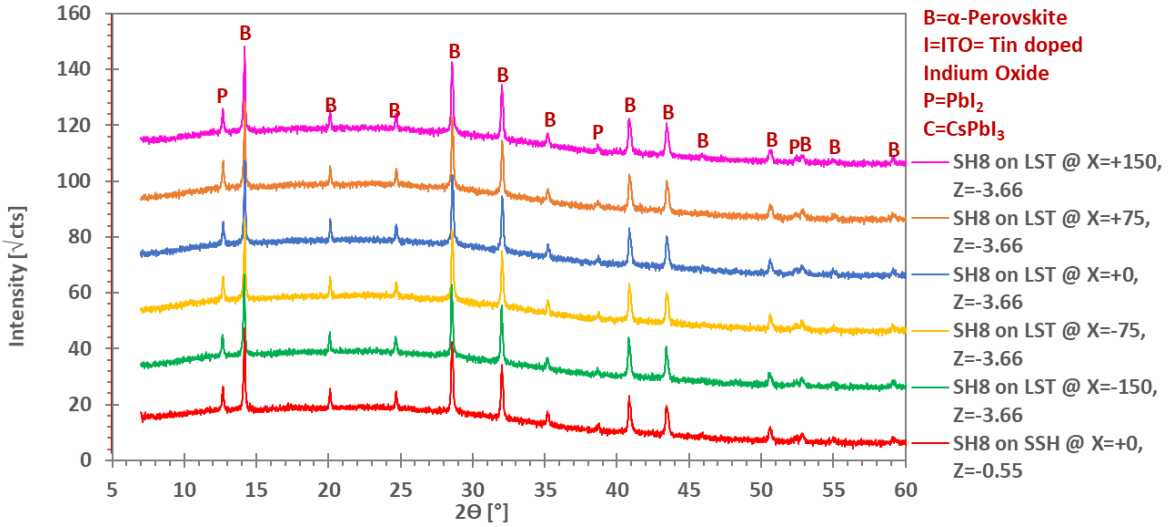

Figure 5. XRD pattern of a slot die coated perovskite sample tested with the Proto-T in the small sample holder (SSH) and on the large sample table (LST) at positions X= 150, 75, 0, -75 and -150 mm.

Figure 5 shows the XRD pattern of a slot die coated perovskite sample tested with the Proto-T in:

- The small sample holder (SSH)
- On the large sample table (LST) at positions X= 150, 75, 0, -75 and -150 mm

The sample consists of almost phase pure α-Perovskite phase ($Cs_xFA_{(1-)x}PbI_{3-y}Br_y$), with a small amount of PbI_2 present. The lattice parameters for the samples are reported in Table 2.

Table 2. Lattice parameters calculated from XRD pattern of a slot die coated perovskite sample tested with the Proto-T in the small sample holder (SSH) and on the large sample table (LST) at positions X= 150, 75, 0, -75 and -150 mm.

		Perovskite				
	Speed	**a [Å]**	**c [Å]**	**Δ2θ [°]**	**Z-error**	**X-position**
Sample	[°/min]				ΔZ [mm]	[mm]
SH8 on LST @ X=+150	7.80	8.8326	10.8174	-0.0024	0.007	150
SH8 on LST @ X=+75	7.80	8.8302	10.8111	-0.0081	0.019	75
SH8 on LST @ X=+0	7.80	8.8301	10.8139	-0.0105	0.025	0
SH8 on LST @ X=-75	7.80	8.8315	10.8142	-0.0096	0.022	-75
SH8 on LST @ X=-150	7.80	8.8309	10.8180	0.0253	-0.058	-150
SH8 on SSH @ X=0	7.80	8.8302	10.8125	0.0067	-0.015	0

Therefore, accuracy on large areas up to 30 cm in x direction is achieved with the D8 Proto-T unit.

The XRD and HSI tool combination was used to analyse slot die coated perovskite films:

- In situ imaging of the perovskite quenching (HSI)
- Analysis of films with unknown properties: (in-situ with HSI, and at-line with XRD)
- Prediction of film properties: quantification models developed to correlate HSI signal with thickness, roughness, phase composition (characteristic 2θ reflections) and photovoltaic parameters (power conversion efficiency, fill factor).

2.2. In-situ imaging of perovskite quenching

Perovskite films are formed by slot die coating of inks containing precursors in a suitable solvent system and subsequent drying. For use in ambient conditions, green solvents often including additives for optimal rheology and surface tension are used. To obtain high quality films, transition of the wet layer to a solid coating must be accelerated usually via a gas- or vacuum-assisted process. During this quenching phase, nucleation of perovskite is induced. Quenched films are then subdued to an annealing process (thermal treatment) to allow growth of the perovskite crystal grains and removal of residual solvent.

Within NanoQI, a solution was developed to image in real time in-situ the quenching of the perovskite layer, which is the most crucial in perovskite film manufacturing, by installing the HSI cameras on top of a vacuum chamber with transparent window. Representative images recorded with the VNIR (Baldur) and SWIR cameras are reported in Figure 6. The quenching is visualized with the transition from a yellow ink to a brown solid film. The sample moves in the vacuum chamber by transport on the roller conveyor belt. Movement direction is inverted approximately every 12.5 cm travel distance (defined as “stroke”). Transport axis is perpendicular to the scanning line direction (see Figure 7.e for a schematic of the cell and scanning direction). Therefore the HSI scans are a repetition of sample images (alternatively specular to each other), with every repetition corresponding to a stroke.

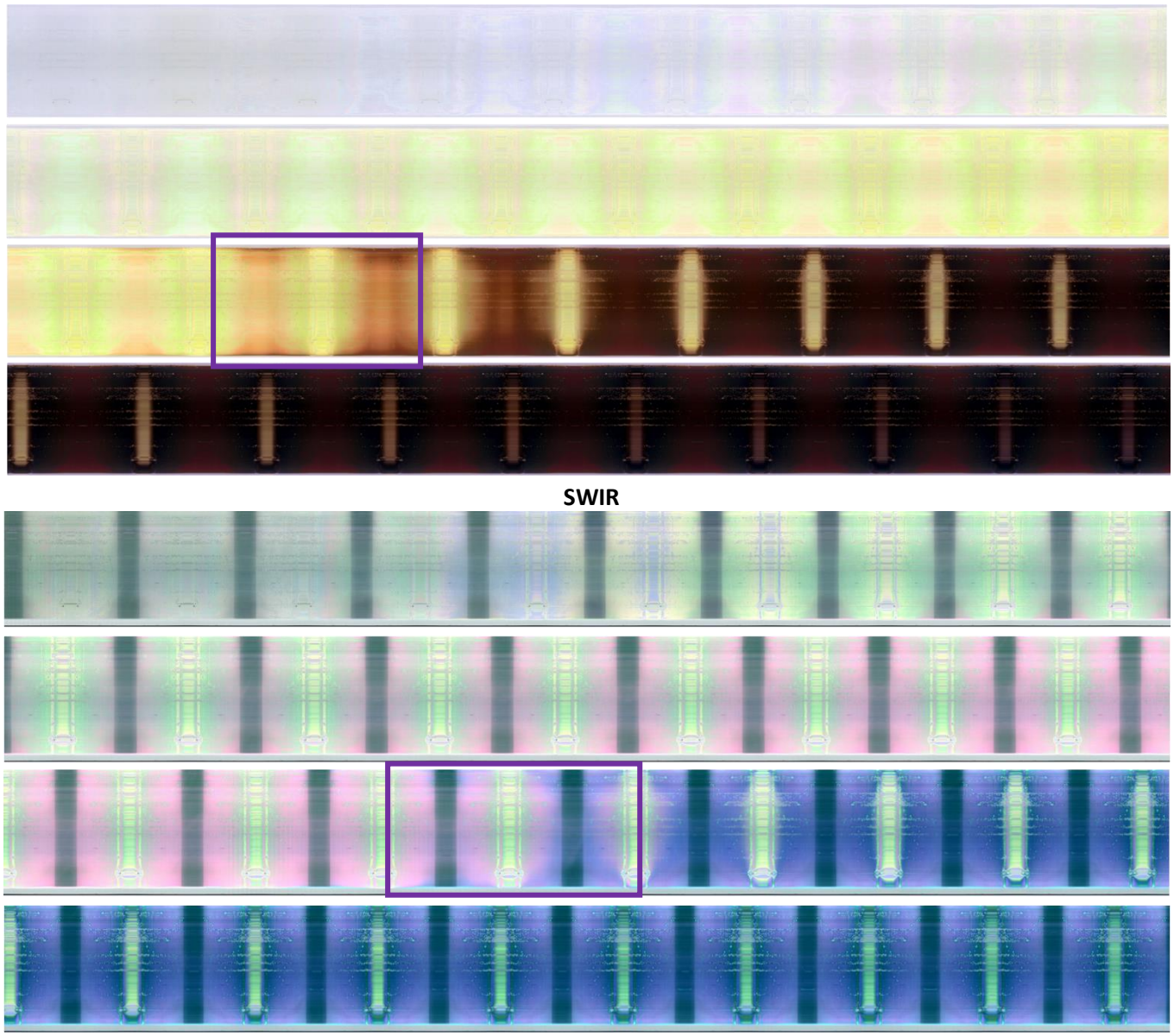

Figure 6. In-situ imaging of the quenching of perovskite films slot die coated on 30 cm x 40 cm substrates. Sample speed is 80 mm/s. Images were recorded simultaneously with the SWIR384 and Baldur-V-1024N cameras.

Analysis of the initial and intermediate phases in the quenching process is not trivial. These phases (liquid film of precursors, intermediate complex of perovskite precursor and solvent) are metastable and convert to secondary (non-photoactive) phases when exposed to air and humidity. Therefore, additional XRD analysis was performed at-line on fully dried samples. In-situ visualization of the quenching process can provide valuable information for quality control in perovskite manufacturing. The vacuum quenching process is characterized by an initial decrease of the pressure in the vacuum chamber (formation of an intermediate complexed phase), followed by its abrupt increase (decomposition of the complexed phase) and consequent decrease (nucleation and growth of perovskite crystals). Based on ambient slot die coating process development at an intermediate platform, optimal quenching state has been identified with the beginning of the second pressure decrease phase. Communication between the HMI of the quenching/curing oven and the HSI software could be in the future implemented to provide inputs on the best time to interrupt the quenching process and proceed with the following ones (refill of the chamber and thermal annealing).

Evaluation of coating with different quenching times is reported in section 2.3. In Figure 7.a and 7.b, imaging of the quenching with the second HSI setup implemented at TNO (SWIR+VNIR1800) is shown. Each image is composed by the repetition of 11 scans of the sample (corresponding to 11 strokes). Perovskite nucleation is observed between stroke 7 and 10.

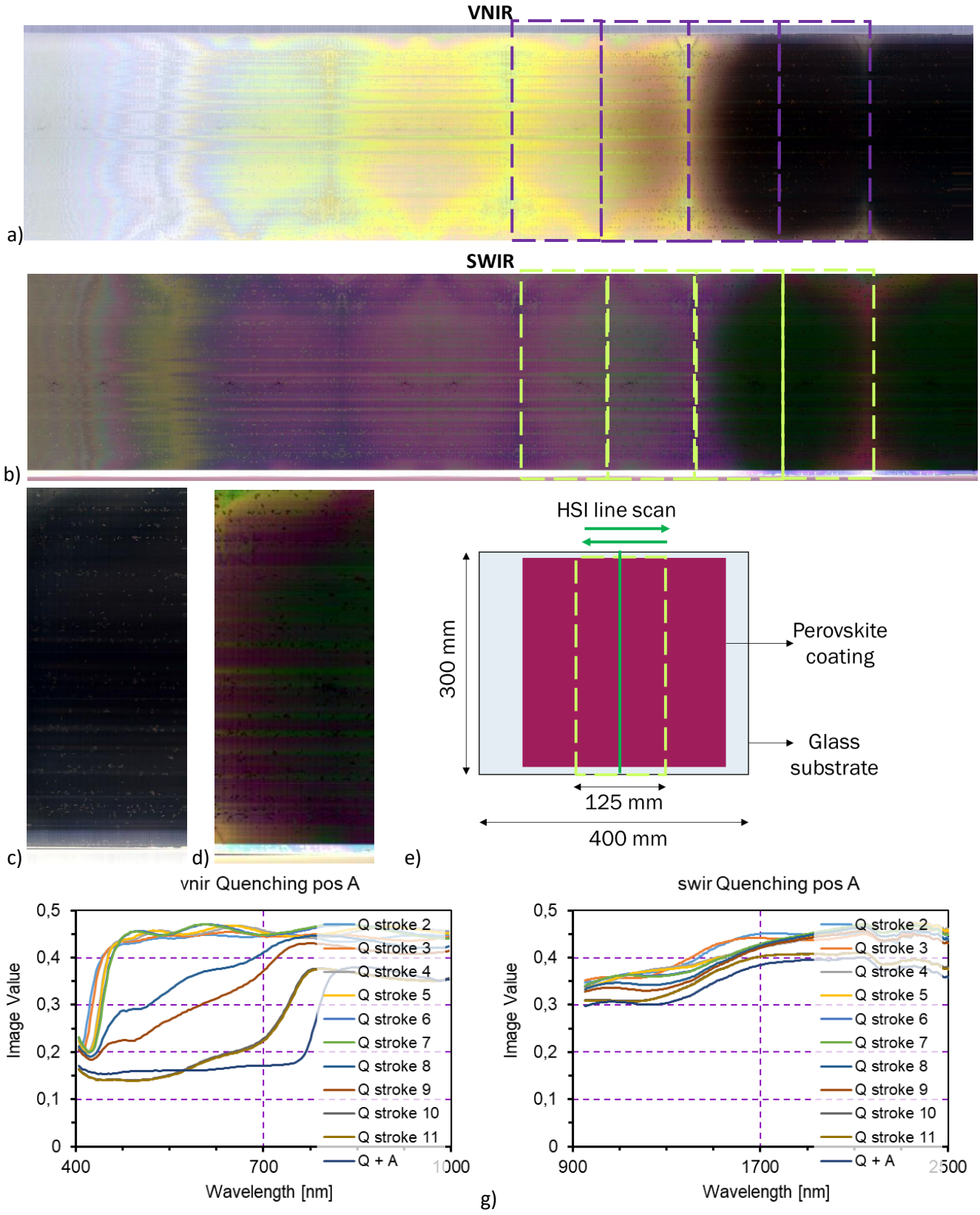

Figure 7. a, b) In-situ imaging of the quenching of slot die coated perovskite films on 30 cm x 40 cm substrates. Incipit of the perovskite nucleation is highlighted. Each dotted square corresponds to a sample scan in the time of a "stroke" (approx. 12,5cm movement). c, d)HSI images of the coatings in a and b recorded after quenching and annealing; f, g) reflection spectra obtained from HSI images of the coatings at different quenching time and after complete quenching and annealing. Position A is at the centre of the samples. e) schematic of the perovskite coatings imaged with the HSI. Images were recorded at a sample speed of 14 mm/s with the a, c, f) VNIR1800 and b, d, g) SWIR384 cameras.

Figure 7.c and 7.d show the VNIR and SWIR images of the quenched samples in 7.a and 7.b after thermal annealing of the coatings (15 min at 140°C). The evolution of the reflection values ad a function of the quenching time and after quenching and subsequent annealing treatment are reported in Figure 7.f and 7.g. A clear variation in the reflection is observed in the VNIR spectral region, especially between 450 and 800 nm. The onset of the perovskite absorption is in fact located at 800 nm/ Marked variations in the optical features of the coatings can be observed also in the SWIR spectral region.

2.3. Thickness and roughness models

Perovskite samples were slot die coated, quenched and annealed to evaluate and develop models to predict morphological variations with the HSI setups. Thickness and roughness values were selected as properties of interest. The film thickness was varied by changing the ink feed in the slot die process. Being a solution-based process, uniform deposition and accurate control of the thickness over large areas is challenging. Therefore, thickness and roughness of the coated films was measured with a profilometer on several locations of each sample (see Figure 8 and Table 3).

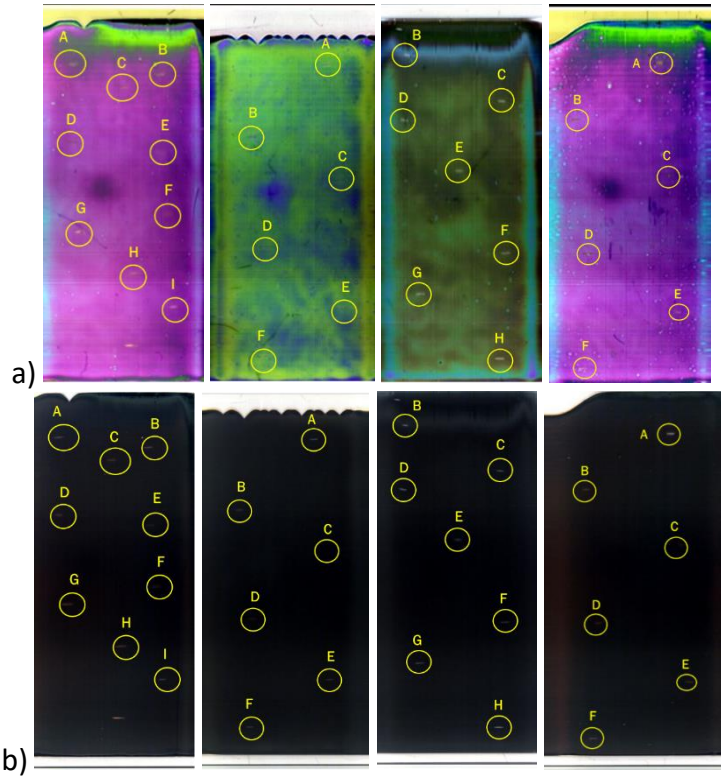

Figure 8. a) SWIR and b) VNIR HSI images of perovskite coatings on 30 cm x 30 cm substrates. Imaged area is approx. 12.5 cm x 30 cm. Sample positions were thickness and roughness used for quantification model were measured are marked in yellow.

Table 3. Thickness and root mean square roughness (Rq) of slot die coated perovskite samples in Figure 8.

	Thickness(nm)				*Root mean square roughness (nm)*			
Position	SM5	SM6	SM4	SM2	SM5	SM6	SM4	SM2
A	488	738		514	10.3	14.2		9.7
B	473	727	1253	407	9.3	12.6	23.8	9.5
C	463	736	1080	428	9.5	12.0	18.3	10.3
D	427	731	1080	410	9.2	11.4	20.5	11.8
E	410	719	1049	413	6.8	13.2	17.0	12.9
F	403	679	1057	400	8.4		20.9	
G	367		1094		13.4		18.7	
H	429				9.1			
I	376				11.5			

The software Breeze, with license provided by NEO, was used for calculation of a partial least square (PLS) quantification model correlating HSI signals to thickness and roughness. Sample areas of interest were selected via manual segmentation. Some samples were used to train the model, while others were used as unknown test samples to evaluate the prediction quality of the model. The model generated for correlation of the SWIR HSI signal with the film thickness is shown in Figure 9. The "Overview (Total for all Y)" graph shows the quality of the PLS model, together with the number of components used by the autofit. R2 (model fit) and Q2 (prediction from cross-validation) of 1.0 indicate a perfect model explaining all the variations. A value of 0 indicates that no variation can be explained.

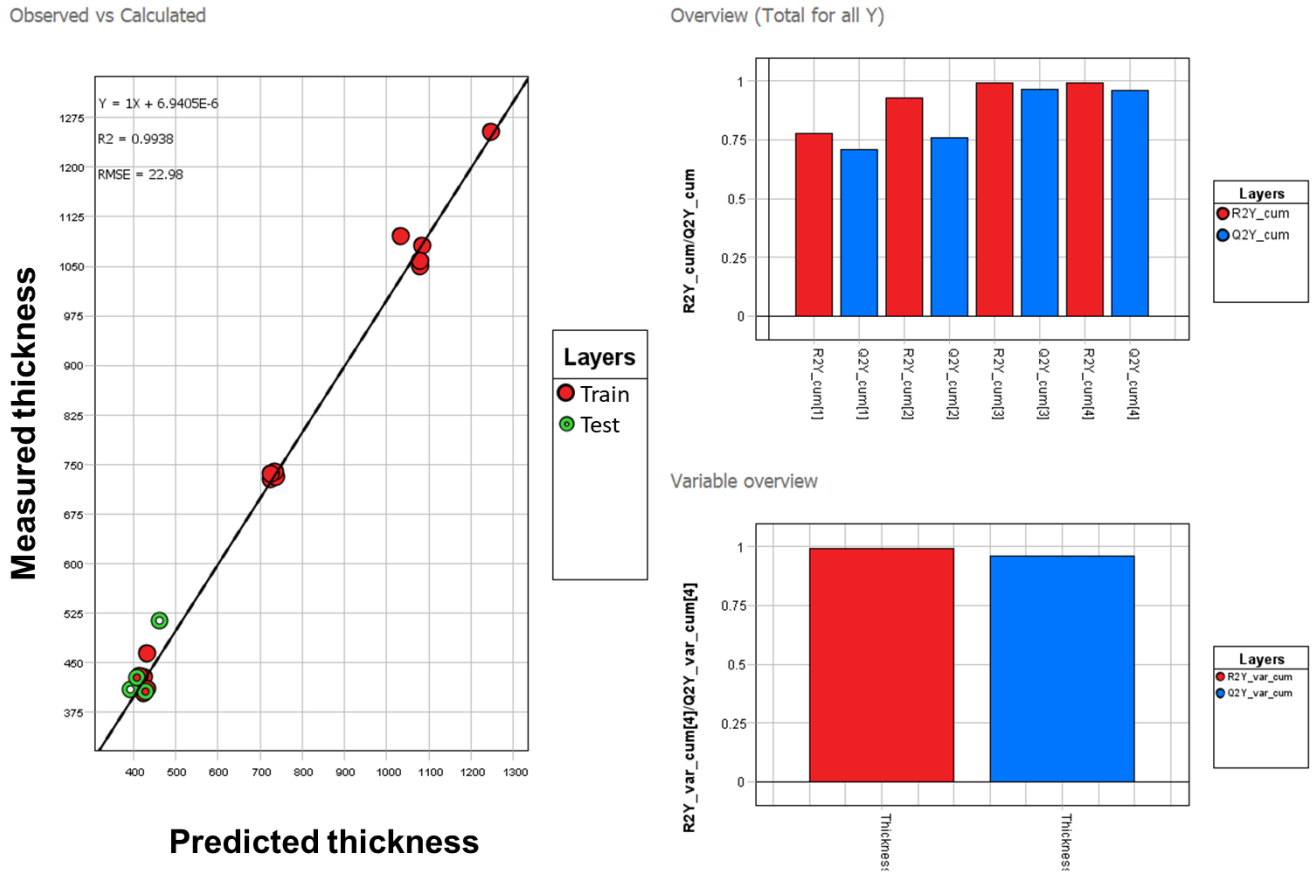

Figure 9. PLS quantification model correlating SWIR HSI data and sample thickness. The model was built with 18 samples, 277 wavelengths, and 4 components.

A very good model was built for the SWIR-HSI – thickness correlation, with R2 and Q2 values of 0.99 and 0.96 respectively. The same is valid for the correlation between VNIR-HSI and thickness, shown in Figure 10. For this model R2 and Q2 were 0.99 and 0.98 respectively.

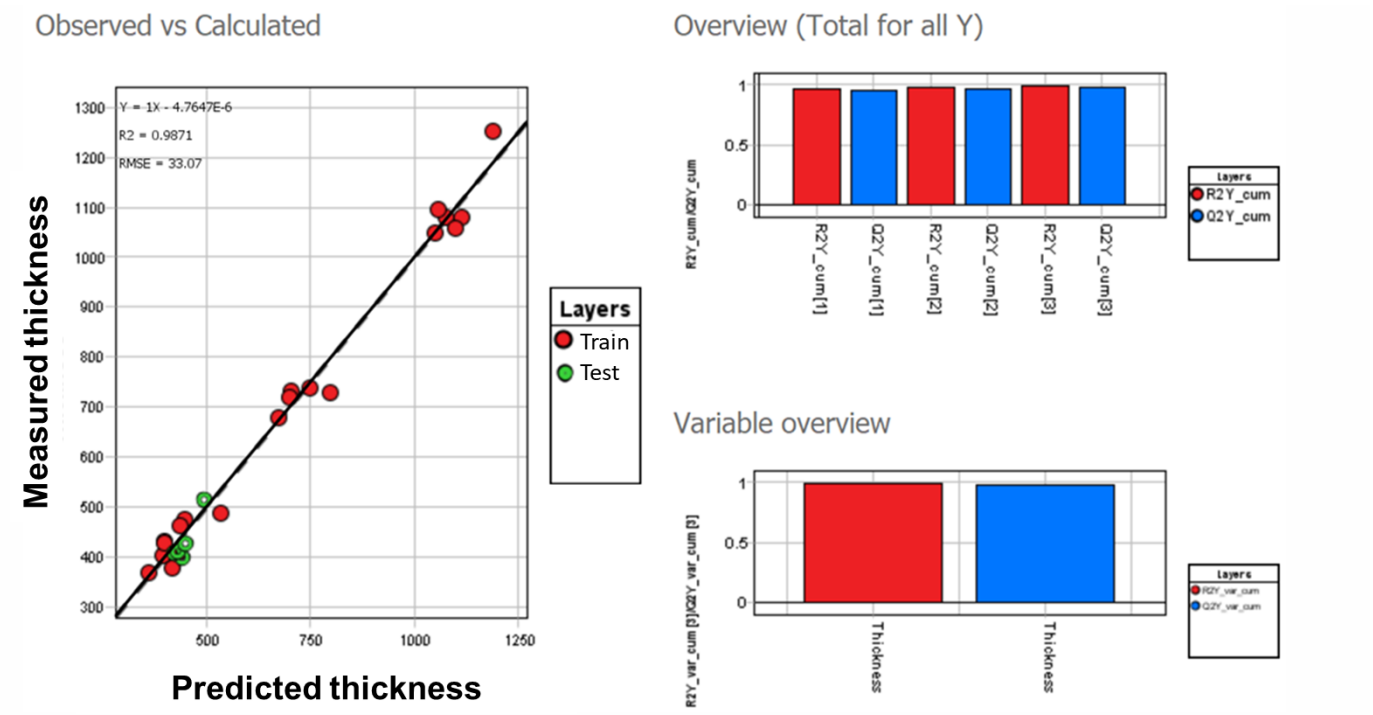

Figure 10. PLS quantification model correlating VNIR-HSI signal and film thickness. Model was generated using 26 samples, 69 wavelengths and 3 components.

The PLS models for the roughness, based both on SWIR (Figure 11.a) and VNIR data (Figure 11.b), demonstrated slightly less accuracy in value prediction: R2 and Q2 are 0.94 and 0.77 respectively for the SWIR, and 0.87 and 0.76 respectively for the VNIR. Finer tuning is advised for these models, although they already provide satisfying value prediction, for example by including larger variations in roughness values in the data set.

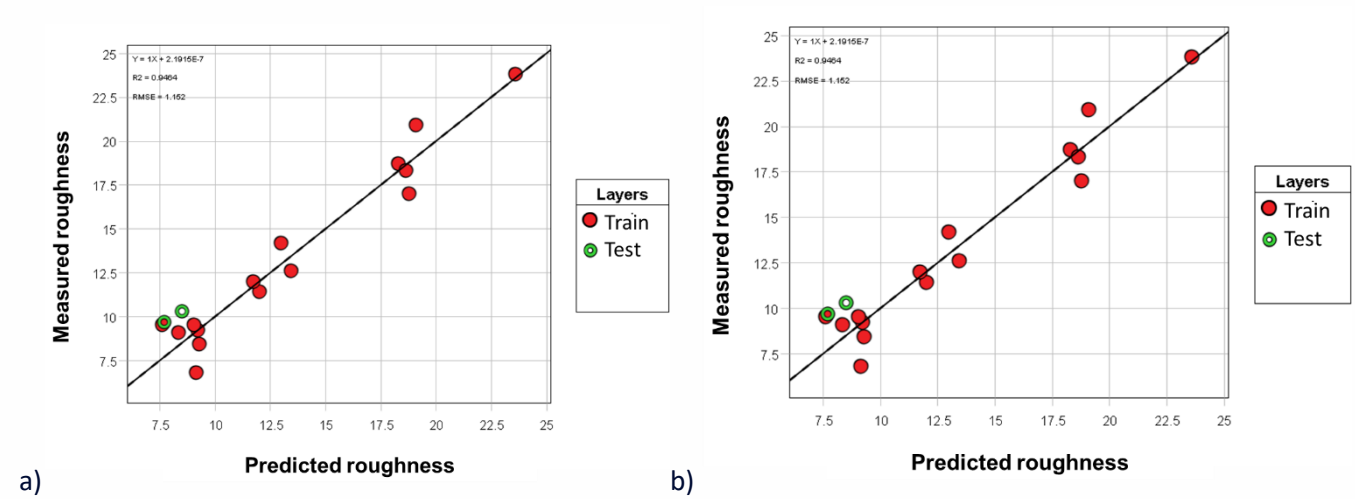

Figure 11. Measured versus predicted roughness values according to PLS quantification models based on a) SWIR and b) VNIR HSI data of slot die-coated large-area perovskite samples.

2.4. Composition model

Experiments were designed to develop a model correlating the composition of perovskite coatings to their HSI characteristics. Due to the nature of solution processed perovskite coatings, preparing films with controlled gradients in perovskite composition was identified as a non-viable route. When changing the composition of the perovskite ink, the crystallization, morphology and amorphous material percentage are in fact also affected. The

perovskite ink is composed of PbI_2, CsBr and FAI dissolved in a green solvent-based mixture containing organic additives. Phases of interest in the XRD spectra of perovskite samples are:

- $CsPbI_3$ (orthorhombic)
- $FAPbI_3$ (yellow, δ-perovskite hexagonal phase)
- $FAPbI_3$ (black, α-perovskite hexagonal phase)
- PbI_2

However, other intermediate or complexed phases, for example with residual solvent molecules, might also be present in the perovskite XRD pattern, complicating the analysis of non-optimally quenched perovskite coatings. To establish a correlation between HSI and characteristic XRD peaks, at first samples with inhomogeneous perovskite crystallization along the film were analysed. The non-optimal properties of the film were obtained by intentionally selecting coating parameters resulting in non-uniform ink distribution or similarly by choosing quenching/annealing settings resulting in partially converted perovskite films, meaning that precursors and or/solvent (complexes) remain in the coated perovskite film. SWIR and VNIR HSI images and XRD analysis of the coatings are shown in Figure 12.

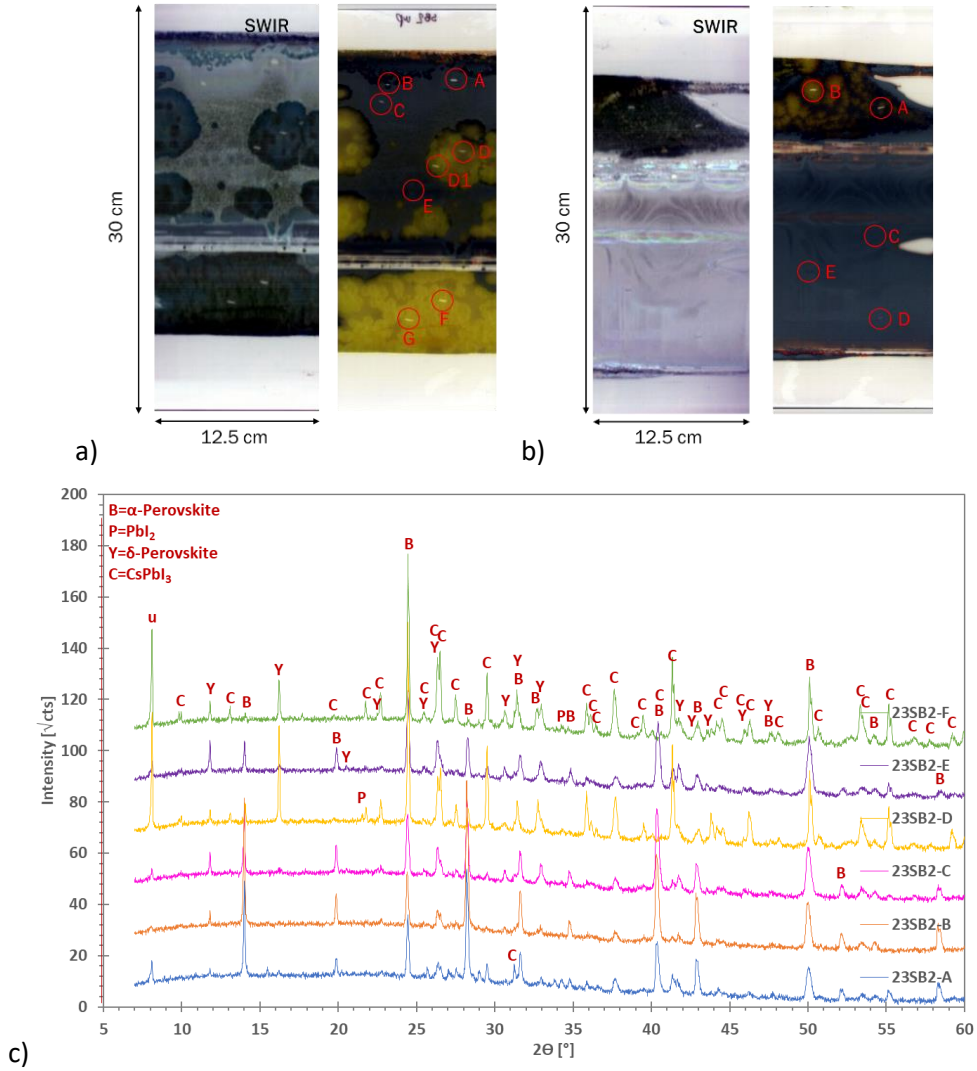

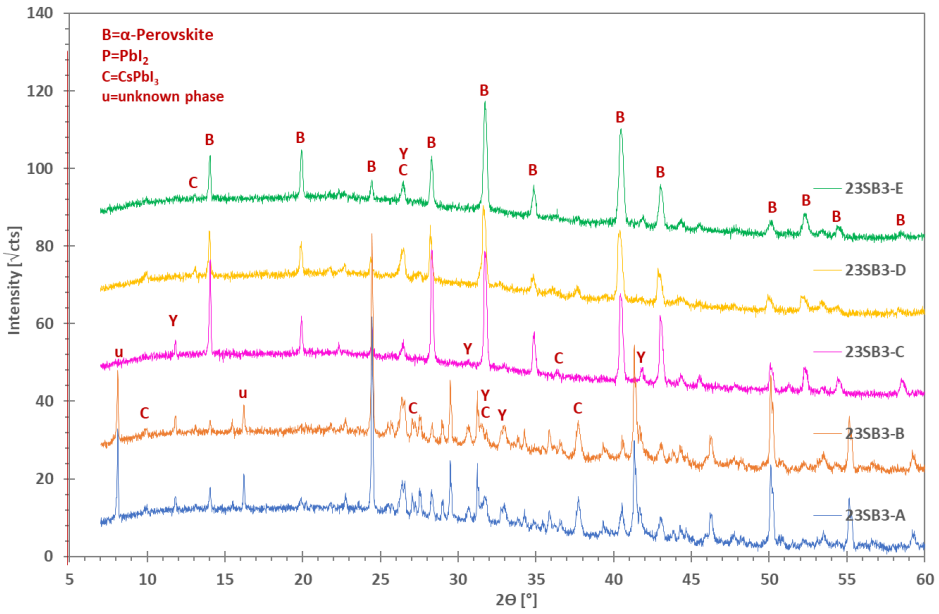

d)

Figure 12: HSI images (SWIR right and VNIR left) of a) 23SB2 and b) 23SB3 slot die coated perovskite samples and c), d) respective XRD patterns.

The XRD patterns of inhomogeneous coatings are complex and include reflections of desired α-perovskite phase (characteristic peaks for example at 2ϑ=14° and 28°) together with undesired PbI_2 and $CsPbI_2$ phases. Peaks of an unknown phase, attribute to an intermediate perovskite complex, are also present (characteristic reflections at 2ϑ=8° and 16°). Pattern interpretation is more complex at certain 2ϑ angles where reflections of different phases overlap (for example 2ϑ=20.6° and 24°). For the quantification models, peak intensity of the reflections at 2ϑ=8°, 14° and 24° were selected as properties. The best correlation was found with the intensity of the peak at 2ϑ=8° (unknown intermediate phase, possibly a solvent-complex phase) which is indicative of non-photoactive perovskite material. The HSI vs XRD models show R2 and Q2 of 0.91 and 0.88 respectively for the SWIR and 0.95 and 0.86 respectively for the VNIR. These are decent models that can be further implemented by increasing the size of the data set. Predicting the intensity of unknown undesired phases seems viable with the HSI-XRD setup developed within NanoQI.

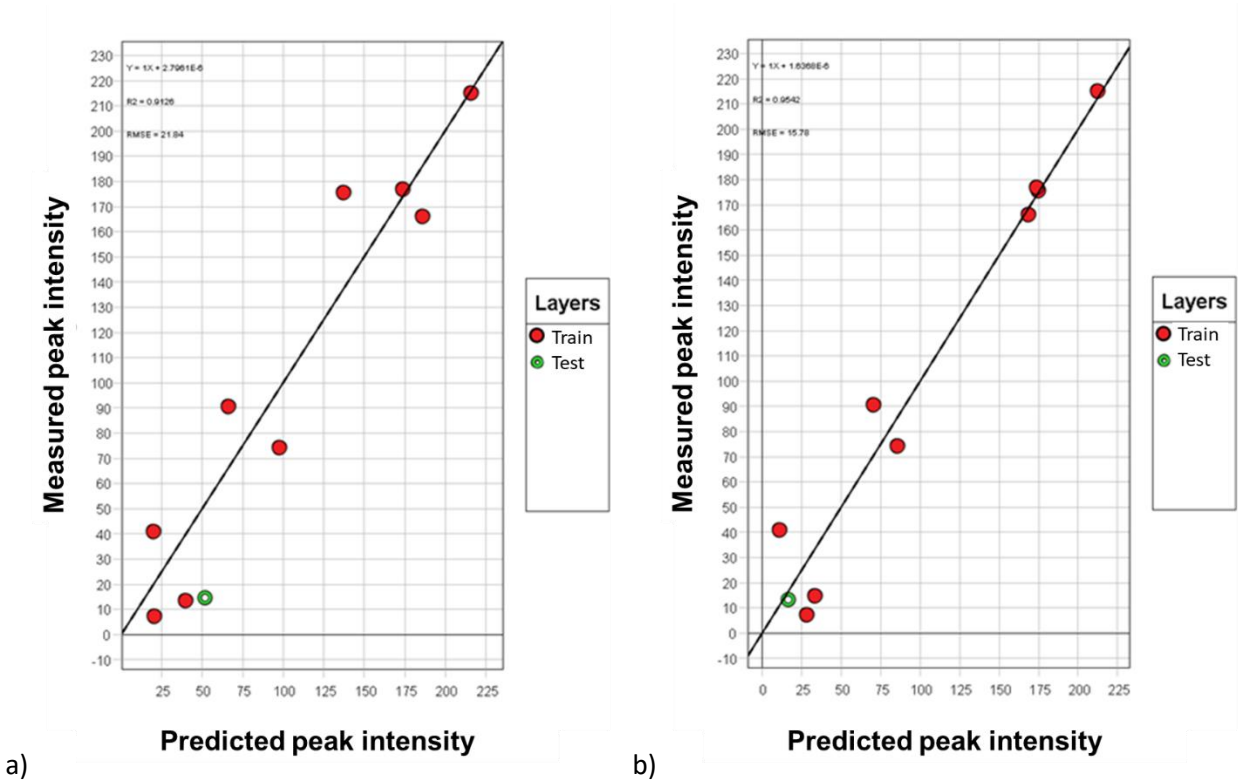

Figure 13. Results of PLS quantification models correlating peak intensity of XRD reflection at 2ϑ=8° with a) SWIR (2 components, 288 wavelengths) and b) VNIR (3 components, 77 wavelengths) signals.

Additionally, models were developed based on series of samples characterised by:

- Different quenching and annealing conditions ((Figure 14). Variations include: no quenching (annealing only) and quenching for different times (followed for all samples by thermal annealing at 140℃); the scope of interrupting the vacuum treatment at different stages of the perovskite crystal formation was to induce formation of different percentages of characteristic crystalline phases in the film.
- Different degradation level. Gradients in degradation of the perovskite coatings was obtained by controlled exposure of fully dried large area perovskite coatings to light, air and moisture with partial coverage of areas of the film during the test; temperature of the films was also monitored during the test to evaluate the presence of degradation due to high temperatures.

Interestingly, the phase at 2ϑ=8° could not be detected in the coatings despite the variability in quenching and annealing conditions and the gradients in degradation time. Therefore, the peak at 2ϑ=14°, which is characteristic of the desired α-perovskite phase, was selected as property of interest for model development after screening of other characteristic peaks present in the XRD pattern of the samples (quality of some models was for example evaluated also in correlation with the peak at 20°.

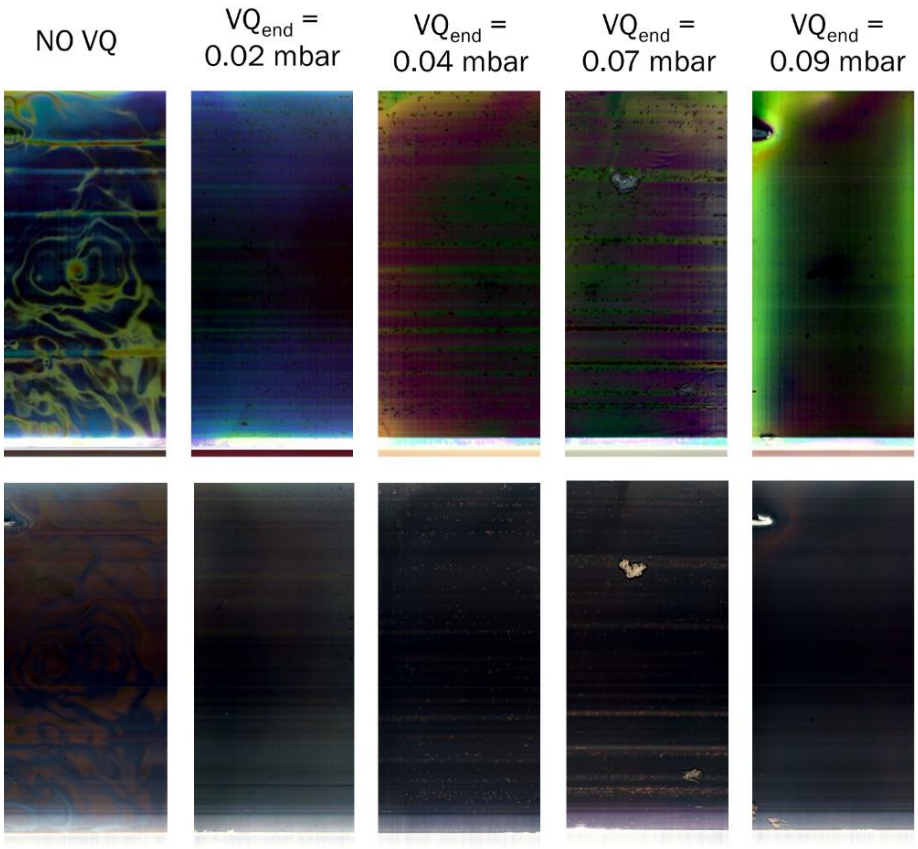

Figure 14. SWIR (top) and VNIR (bottom) HSI images of perovskite coatings (scanned size approx. 30 cm x 12.5 cm) with different quenching state; pressure reached in the vacuum chamber during the quenching step is reported in the figure.

The models yield decent results and are built on a larger data set, see Figure 15. For the prediction of the intensity of the α-perovskite peak, the VNIR produces more accurate results (R2 and Q2 of 0.87 and 0.67) compared to the SWIR (R2 and Q2 of 0.81 and 0.61).

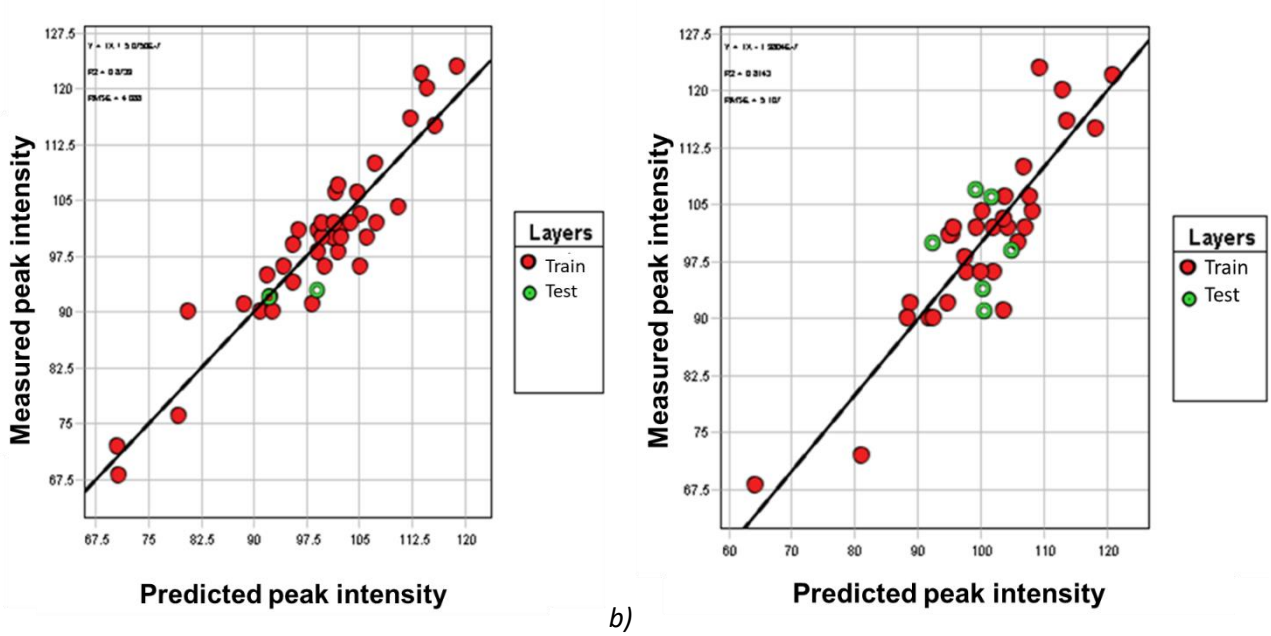

Figure 15. Results of PLS quantification models correlating peak intensity of XRD reflection at 2ϑ=14° with a) SWIR (6 components, 288 wavelengths) and b) VNIR (5 components, 186 wavelengths) signals over 41 samples.

In conclusion, it was possible to build quantification models based on VNIR and SWIR HSI and XRD data for perovskite coatings, based on characteristic reflections of both undesired and desired crystalline phases.

2.5. Solar cell fabrication and evaluation

As a final step of the tool validation, perovskite films deposited by slot die coating on large areas were used to fabricate semitransparent perovskite solar cells with p-i-n architecture. For this purpose, patterned glass/ITO was used as substrate. The films were firstly coated by slot die with a hole transport layer and then with the perovskite precursor ink, followed by quenching and annealing. The same stack was used for all the samples described in this report. Both during quenching and after complete annealing, the coatings were imaged with the SWIR and VNIR cameras. Samples were then cut to 3 cm x 3 cm size, and the stack finalized with a fullerene layer, SnO_2 and a top transparent contact. Each 3 cm x 3 cm substrate includes 4 cells. Devices were measured under solar simulator at standard test conditions (STC) with a metallic aperture mask defining an active area of 0.09 cm^2. Cell architecture and a schematic of the cell pattern on the large area coating are shown in Figure 16. Variation in thickness and in the quenching states were evaluated.

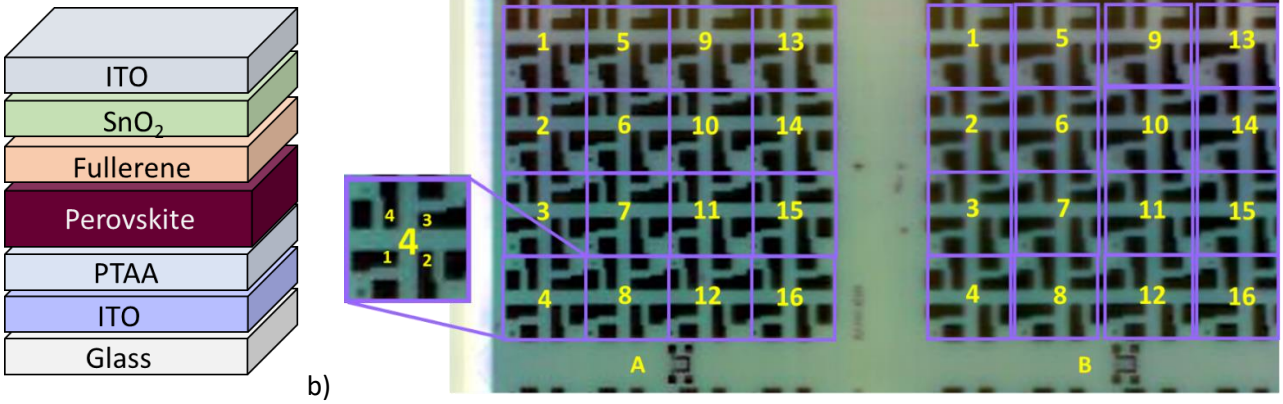

Figure 16. a) Schematic of the perovskite solar cell architecture; b) SWIR HSI image of perovskite coated on glass/ITO (patterned)/PTAA, showing the distribution of the cells on the substrate (128 for each 30 cm x 30 cm plate).

In Figure 17, the manual segmentation to select the cell area (overlap between bottom and top electrode) is represented. 216 cells were fabricated and measured, and their performance parameters were used to build a PLS model. SWIR and VNIR signals were correlated to the power conversion efficiency (PCE) and fill factor (FF) of the cells.

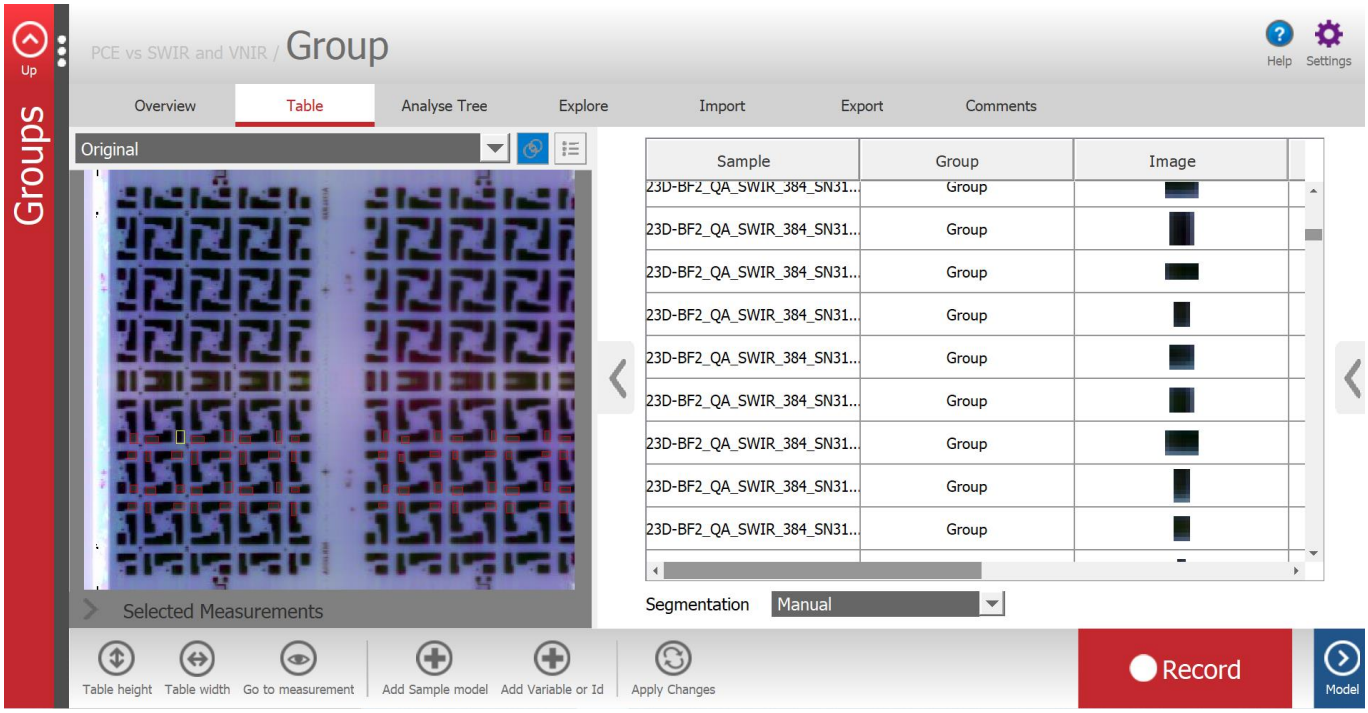

Figure 17. Manual segmentation to select cell active area in the HSI images via the software Breeze

The quantification models could not establish a satisfactory correlation between HSI signal and solar cell performance (either PCE or FF). The best model developed, between SWIR and cell FF, based on 120 cells belonging to the quenching variation sample series, yielded a poor R2 and Q2 of 0.44 and 0.15 respectively, meaning that the behavior of only 15% of the cells can be explained by the model. Calculated vs predicted FF values are reported in Figure 18 together with the statistical distribution of the measured FF.

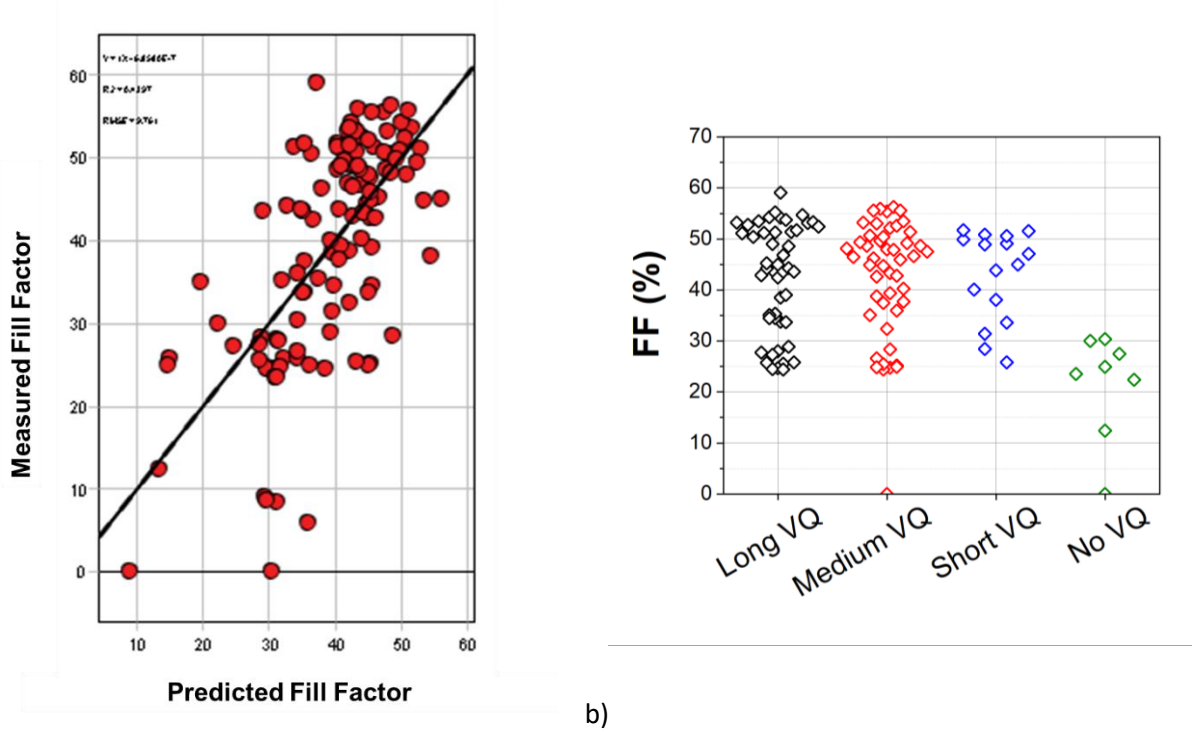

a) b)

Figure 18. a) Calculated vs predicted FF according to the PLS quantification model built based on the SWIR HSI signals of the perovskite layers of 122 small area cells; b) statistical distribution of the FF measured under solar simulator at standard testing conditions (AM1.5G, 1 sun, 25C).

The unfeasibility of developing a reliable model linking the optical properties of the film and the solar cell performance parameters was linked to several challenges to be addressed in the future as possible continuation and follow up of the work carried out in the NanoQI project:

- The models developed consider only optical properties of the films; these are not the only factors affecting the performance of a photovoltaic device, which also depends on electrical and morphological properties of the stack and the layers in the stack.
- Variations in the film morphology, for example presence of defect and pinholes, could be below the resolution limit of the HSI tools, and therefore not considered in the model even though affecting largely the device performance.
- The solar cells stack is combination of multiple layers and the efficiency of the cells is influenced by the quality and homogeneity of all the layers constituting the stack. The models here developed only evaluate stack characteristics up to the perovskite layers, without taking into account the effect of the top electron transport layer, buffer layer and transparent electrode.
- Due to the nature of the perovskite manufacturing process, an overlap between several variables affecting the cell performance is expected for the different samples analyzed, such as thickness and phase composition. These properties might influence the cell performance and the HSI signal to different extents, making it difficult for the model to discriminate between these variables and create a reliable property correlation.
- Measurement instability is a well-known issue of perovskite solar cells. During the current density-voltage (J-V) scans of the cells, a different behavior was sometime observed for cells on the same substrate. Some cells showed a small increase in performance after the scans, while for others a decrease in efficiency was observed. The values used for the model were taken from the third J-V scan for all the cells and are therefore an indication not only of the quality of the stack but also of its stability under light soaking, which shows some cell-to-cell variability.
- The data set selected for the models might not be large or good enough to represent large variations in the cell's performance.

Based on this considerations, further work should be carried out to tune and optimize the HSI vs cell performance models, for example by using more suitable perovskite cell stacks (e.g., improved light stability) or by better controlling the deposition process to achieve uniform distribution of variables along the coating.

3. Conclusions

The NanoQI analytical tool, including an in-situ double camera HSI setup and the customized XRD Proto-T unit, has been demonstrated for application in perovskite solar cells manufacturing. Perovskite coating on 30 cm x 40 cm substrates have been imaged at speeds > 0.5 m/min; an imaging size > 20 cm x 20 cm has been demonstrated.

The feasible measurement speeds of the Proto-T XRD unit has also been assessed and the accuracy over large areas has been verified with both reference materials and perovskite samples.

Films with variation in characteristic properties were fabricated and analysed with the HSI and XRD tools in order to develop prediction models for quality control purposes. Properties of interest that were investigated in this WP included thickness, roughness and phase composition.

To achieve controlled variation in the phase percentage, quenching and annealing variations were evaluated together with controlled ageing of the coatings. Several quantification models were developed:

- Morphology. Quantification models were successfully built to correlate the sample thickness to the HSI data, with excellent results for both the VNIR and SWIR cameras. Good results were obtained also for models correlating HSI signals with roughness of the film, although finer model tuning is advised to enlarge the variations predicted by the models.
- Composition. The intensity of selected XRD peaks was successfully correlated to the VNIR and SWIR HSI data of perovskite coatings. Models showed very good prediction capabilities when the peak of an unknown undesired intermediate phases (perovskite-solvent complex phase) is chosen as property for correlation. Good models could be developed also when evaluating the intensity of XRD peaks characteristic of the desired α-perovskite phase.
- Cell performance. Solar cells were fabricated, and a tentative model was developed to correlate photovoltaic parameters to the HSI signal of the perovskite coatings in the stack. These models could not predict with high accuracy the photovoltaic parameters of the cells. Issues to be addressed in order to improve the models include: increasing the resolution of the analytical tools; preparing coating with a marked separation between variables affecting the cell performance (e.g. uniform composition over the coating and thickness variation) which is technologically still challenging for solution processed perovskite films; overcoming measurement instability; improving homogeneity of all the films in the multi-layered stack.

In this work package the NanoQI analytical tool was used to monitor perovskite film properties during the fabrication process. It was shown that hyperspectral imaging is a perfect tool to measure crucial parameters that are directly linked to the optical properties, such as: thickness, roughness, nucleation, and parasitic phases. However, predicting the solar cell performance based on these parameters has proven to be challenging and requires more data.

Despite these specific challenges, the NanoQI analytical tool is an excellent validation tool for coating properties prediction and has the potential to become a routine characterization setup for perovskite solar cell manufacturing in sheet-to-sheet and roll-to-roll production lines.

4. Degree of progress

Degree of fulfilment is 100%.

5. Dissemination level

This Deliverable is Public.